Virology 528 (2019) 89–100

Contents lists available at ScienceDirect

Virology

journal homepage: www.elsevier.com/locate/virology

Density-dependent enhanced replication of a densovirus in *Wolbachia*-infected *Aedes* cells is associated with production of piRNAs and higher virus-derived siRNAs

Rhys Parry, Cameron Bishop, Lachlan De Hayr, Sassan Asgari*

Australian Infectious Disease Research Centre, School of Biological Sciences, The University of Queensland, Brisbane, QLD 4072, Australia

ARTICLE INFO

Keywords:
Wolbachia
Densovirus
Aedes aegypti
Aedes albopictus
piRNA
RNAi
Short interfering RNA
Mosquito

ABSTRACT

The endosymbiotic bacterium *Wolbachia pipientis* has been shown to restrict a range of RNA viruses in *Drosophila melanogaster* and transinfected dengue mosquito, *Aedes aegypti*. Here, we show that *Wolbachia* infection enhances replication of Aedes albopictus densovirus (AalDNV-1), a single stranded DNA virus, in *Aedes* cell lines in a density-dependent manner. Analysis of previously produced small RNAs of Aag2 cells showed that *Wolbachia*-infected cells produced greater absolute abundance of virus-derived short interfering RNAs compared to uninfected cells. Additionally, we found production of virus-derived PIWI-like RNAs (vpiRNA) produced in response to AalDNV-1 infection. Nuclear fractions of Aag2 cells produced a primary vpiRNA signature U_1 bias whereas the typical "ping-pong" signature (U_1 - A_{10}) was evident in vpiRNAs from the cytoplasmic fractions. This is the first report of the density-dependent enhancement of DNA viruses by *Wolbachia*. Further, we report the generation of vpiRNAs in a DNA virus-host interaction for the first time.

1. Introduction

Aedes aegypti densovirus (AaeDNV) and Aedes albopictus densovirus (AalDNV) are small non-enveloped, single-stranded DNA viruses belonging to the monosense *Brevidensovirus* genus of the *Parvoviridae* family (Bergoin and Tijssen, 2010). Brevidensoviruses have a 4-kb genome with three open reading frames on the same strand encoding for two non-structural proteins (NS1, NS2) and a capsid protein (VP) (Bergoin and Tijssen, 2010), as well as a small ORF with unknown function on the complementary strand (Afanasiev et al., 1991). Unique palindromic sequences of approximately ~140–160 nt at the 3′ and 5′ ends of the genome fold to form a T-shaped structure (Afanasiev et al., 1991). Densoviruses replicate and form paracrystalline arrays in the nuclei of mosquito cells and cause a characteristic nuclear hypertrophy (densonucleosis) (Carlson et al., 2006).

AaeDNV, AalDNV and also Anopheles gambiae densovirus (AgDNV) have been extensively studied as transducing vectors and biocontrol agents (Reviewed by Carlson et al. (2006); Johnson and Rasgon (2018)). Both *Aedes aegypti* and *Aedes albopictus* are vectors of a diverse range of medically-relevant viruses from the *Togaviridae* and *Flaviviridae* families such as chikungunya virus (CHIKV), dengue virus (DENV) and Zika virus (ZIKV) (Bhatt et al., 2013; Juliano and Lounibos, 2005). Aedes densoviruses are attractive biocontrol agents as both AaeDNV and AalDNV have been demonstrated to be infectious to all life stages of mosquito hosts and unable to infect other insect or mammalian hosts (Jousset et al., 1993). Experimental infection of *Ae. aegypti* and *Ae. albopictus* mosquitoes with AaeDNV and AalDNV causes a spectrum of pathological effects on the mosquito host.

AalDNV has been demonstrated to cause up to 97.6% mortality in the first instar *Ae. aegypti* larvae (Barreau et al., 1996), whereas AaeDNV has been shown to cause 66% and 64% larval and pupal mortality in *Ae. aegypti* and *Ae. albopictus*, respectively (Buchatsky et al., 1997). Aedes Thailand densonucleosis virus (AThDNV) was demonstrated to produce a larval mortality rate of 51% and 82% in *Ae. aegypti* and *Ae. albopictus*, respectively (Kittayapong et al., 1999). Further examination of AaeDNV-induced mortality in *Ae. aegypti* mosquitoes by Ledermann *et al.* suggested that mortality is a dose-dependent effect with peak mortality of up to 75% (Ledermann et al., 2004). Horizontal transmission of AalDNV and AaeDNV in the wild aquatic environments is thought to occur from larvae to larvae, and also venereal transmission has been demonstrated between adult mosquitoes (Barreau et al., 1997). Additionally, transovarial transmission has also been demonstrated in a large cage trial of AaeDNV in *Ae. aegypti* mosquitoes (Wise de Valdez et al., 2010).

Wolbachia pipientis is a gram-negative endosymbiotic bacterium present in 40–65% of insect species, diverse arthropods and nematodes

* Corresponding author.
E-mail address: s.asgari@uq.edu.au (S. Asgari).

https://doi.org/10.1016/j.virol.2018.12.006
Received 11 October 2018; Received in revised form 20 November 2018; Accepted 5 December 2018
Available online 22 December 2018
0042-6822/

(Hilgenboecker et al., 2008; Jeyaprakash and Hoy, 2000). Endosymbiotic *Wolbachia* infections of *Drosophila melanogaster* have been demonstrated to reduce viral loads when challenged with dsRNA and positive sense RNA viruses (Hedges et al., 2008; Teixeira et al., 2008). Despite the ubiquitous presence of *Wolbachia* within insect hosts, a worldwide survey of *Ae. aegypti* from 27 countries and six continents showed absence of *Wolbachia* (Gloria-Soria et al., 2018). Only a single report of a naturally occurring infection of *Wolbachia* in *Ae. aegypti* mosquitoes has been published, which suggests that a natural *Wolbachia* infection in *Ae. aegypti* mosquitoes is absent or exceedingly rare (Coon et al., 2016). In contrast, *Ae. albopictus* mosquitoes are naturally infected with two strains of *Wolbachia* (*w*AlbA and *w*AlbB), which can be single infections or superinfections of both strains (Sinkins et al., 1995; Zhou et al., 1998).

Stable introduction of *Wolbachia w*Mel and *w*MelPop from *D. melanogaster* into *Ae. aegypti* mosquitoes and cell lines has been shown to restrict replication and dissemination of medically important single stranded RNA viruses such as DENV, ZIKV, Yellow fever virus, and West Nile virus from the family *Flaviviridae* (Aliota et al., 2016a; Dutra et al., 2016; Hussain et al., 2013a; Moreira et al., 2009; van den Hurk et al., 2012; Walker et al., 2011; Ye et al., 2015), as well as members of *Togaviridae* such as CHIKV and Mayaro virus (Aliota et al., 2016b; Moreira et al., 2009; van den Hurk et al., 2012). Stable transinfection of *w*Mel in *Ae. albopictus* has also been demonstrated to restrict DENV and CHIKV in the mosquito host (Blagrove et al., 2012, 2013). In addition to stable *w*Mel/*w*MelPop transinfections, it has also been demonstrated that stable infection of *Wolbachia* strain *w*AlbB from *Ae. albopictus* into *Ae. aegypti* mosquitoes increases *Ae. aegypti* DENV refractoriness (Ant et al., 2018; Bian et al., 2010; Joubert and O'Neill, 2017; Joubert et al., 2016).

Efforts to determine interactions between *Wolbachia* and the insect host have primarily focused on single-stranded positive-sense RNA viruses. It has been reported that stable transinfection of *w*MelPop-CLA in *Ae. aegypti* Aag2 cells restricts the single-stranded positive-sense RNA virus Cell Fusing Agent virus (CFAV, *Flaviviridae*) (Schnettler et al., 2016; Zhang et al., 2016) but does not restrict the single-stranded negative-sense RNA virus Phasi Charoen-like virus (PCLV, *Bunyaviridae*) (Schnettler et al., 2016) nor the single-stranded negative-sense RNA virus Aedes anphevirus (family not assigned) (Parry and Asgari, 2018) within these cells.

Currently, only two reports have characterised the interaction of *Wolbachia*-infected insects with DNA viruses. *D. melanogaster* infected with *w*Mel showed an increased mortality when challenged with Invertebrate iridescent virus 6 (IIV-6, *Iridoviridae*), compared to the tetracycline cleared fly line (Teixeira et al., 2008). Titration of IIV-6 in challenged flies showed a non-significant 1.8-fold increase in the presence of *Wolbachia* compared to uninfected flies (Teixeira et al., 2008). In the second report, the presence of three different *Wolbachia* strains *w*Exe1, *w*Exe2, and *w*Exe3 in the African armyworm moth *Spodoptera exempta* was positively associated with prevalence of Spodoptera exempta nucleopolyhedrovirus (SpexNPV) related deaths in the moth's larvae (Graham et al., 2012). Laboratory bioassays also demonstrated that the presence of *Wolbachia* increased susceptibility and decreased survival of *S. exempta* challenged with SpexNPV (Graham et al., 2012).

A number of *Aedes* densoviruses have been isolated from persistently infected mosquito cell lines that show no observable cytopathic effects (Boublik et al., 1994; Chen et al., 2004; O'Neill et al., 1995). To examine the possibility of persistent densovirus infection in our Aag2 cell line and also the possible interactions between *Wolbachia* infection and densovirus, we conducted RNA sequencing and also re-analysed small RNA profiles of virus-derived RNAs in Aag2 and Aag2.*w*MelPop-CLA cells produced previously from the cytoplasmic and nuclear fractions (Mayoral et al., 2014a, 2014b). In addition, we also explored the effect of a supergroup B *Wolbachia* strain (*w*AlbB) on Aedes densovirus by generating a stably transinfected Aag2 cell line with *w*AlbB (denoted Aag2-*w*AlbB).

2. Methods and materials

2.1. Mosquito cells

Ae. aegypti Aag2 cell line (Peleg, 1968) and Aag2 cells infected with *Wolbachia pipientis w*MelPop-CLA (Frentiu et al., 2010), *Ae. albopictus* Aa23 cells (O'Neill et al., 1997) and *Ae. albopictus* C6/36 cells (Singh, 1967) were maintained in 1:1 Mitsuhashi-Maramorosch and Schneider's insect medium (Invitrogen) supplemented with 5–10% fetal bovine serum (FBS, Bovogen Biologicals, French origin), while Aa20 cells (Pudney et al., 1979) were maintained in L15 medium (Invitrogen) supplemented with 10% tryptose phosphate broth (TPB) and 5% FBS. All mosquito cell lines were kept at 28 °C and passaged every 3–4 days. Tetracycline treatment of cell lines was conducted as previously described (Asad et al., 2018).

2.2. Production of stably infected Aag2-wAlbB cell line

*Wolbachia w*AlbB strain from *Ae. albopictus* Aa23 cells was transinfected into the Aag2 cell line using a previously described method (Iturbe-Ormaetxe et al., 2011). Briefly, Aa23 cells were maintained in a 1:1 mixture of Mitsuhashi–Maramorosch and Schneider's insect medium (Invitrogen), supplemented with 10% FBS, in a 175 cm^2 culture flask until confluent. Cells were then lysed *via* sonication, and the lysate filtered through a 2.7 μm filter. The filtrate was centrifuged and resuspended in 2 mL of 1:1 Mitsuhashi–Maramorosch and Schneider's insect medium, supplemented with 10% FBS. The suspension was added to 1.5×10^6 Aag2 cells adhered to one well of a 6-well plate, and incubated for 24 h at 27 °C. Cells were then resuspended and maintained in a 1:1 mixture of Mitsuhashi–Maramorosch and Schneider's insect medium, supplemented with 10% FBS, and passaged regularly at high density to increase *Wolbachia* density. Samples were taken at each alternate passage and tested for *Wolbachia* density *via* qPCR targeting the *Wolbachia Surface Protein* gene (*wsp*) (forward: 5′-ATCTTTTATAG CTGGTGGTGGT-3′; reverse:5′ GGAGTGATAGGCATATCTTCAAT-3′) relative to *Aa. aegypti Ribosomal Protein Subunit 17* gene (*RPS17*) copy numbers (forward: 5-CACTCCCAGGTCCGTGGTAT-3′; reverse 5′-GGAC ACTTCCGGCACGTAGT-3′). To generate a *Wolbachia* free Aag2-*w*AlbB line (Aag2-*w*AlbBT), we tetracycline cured the cells using a previously described method (Asad et al., 2018).

2.3. Experimental inoculation of Aa20 cells with AalDNV-1

Aa20 cells were experimentally infected with AalDNV-1 from persistently infected Aag2 and C6/36 cell lines as follows. 6×10^6 Aa20 cells were seeded into a 12-well plate and allowed to adhere for 30 min. To prepare AalDNV-1 inoculum from cell lines, C6/36 and Aag2 cells were spun at 16,000x*g* for 3 min. The supernatant was then filtered through a 0.22 μm filter. Aa20 medium was removed and replaced with 1 mL of inoculation medium. Cells were rocked for 1 h, and the first time point was designated as day 0. Samples were then taken at 1, 3 and 5 days post infection.

2.4. RNA extraction and sequencing

Total RNA of Aag2 cells was extracted using QIAzol Reagent (Qiagen). Total RNA was quantified and qualified by Agilent 2100 bioanalyzer (Agilent Technologies, Palo Alto, CA, USA), NanoDrop (Thermo Fisher Scientific Inc.) and 1% agarose gel. 1 μg total RNA with RIN value above 7 was used for the following library preparation. Next generation sequencing library preparations were constructed according to the manufacturer's protocol using NEBNext First Strand Synthesis Reaction Buffer and NEBNext Random Primers. First-strand cDNA was synthesized using ProtoScript II Reverse Transcriptase and the second-strand cDNA was synthesized using Second Strand Synthesis Enzyme Mix. The purified double-stranded cDNA (by AxyPrep Mag PCR Clean-

up, Axygen) was then treated with End Prep Enzyme Mix to repair both ends and add a dA-tailing in one reaction, followed by a TA ligation to add adaptors to both ends. Size selection of adapter-ligated DNA was then performed using AxyPrep Mag PCR Clean-up, and fragments of ~360 bp (approximate insert size of 300 bp) were recovered. Each sample was then amplified by PCR for 11 cycles using P5 and P7 primers. Samples were sequenced by Genewiz.

2.5. DNA extraction and PCR amplification

DNA was extracted using a DIY spin column protocol as previously described (Ridley et al., 2016). A primer was designed to amplify a 298 bp region of the AalDNV-1 NS1 protein (forward: 5′-AGTGAACAT TCGCCGTGTGA-3′; reverse 5′-CTCTGGAGCCGCTGTGTAAT-3′). Three-step qPCR with melt curve analysis was undertaken using QuantiFast SYBR Green PCR Kit (QIAGEN, Germany) and using a Rotor-Gene Q machine (QIAGEN, Germany) with 200 ng of input DNA (5 µL SYBER Green, qF/qR primer 0.25 µL, H_2O 0.5 µL). Amplification was performed at 95 °C for 1 min, followed by 35 cycles of 95 °C for 30 s, 56 °C for 30 s, 68 °C for 1 min and a final extension at 68 °C for 5 min. Control primers for host were the *Ae. aegypti RPS17* gene and also the *wsp* gene for *Wolbachia*. All PCR products were individually inspected using melt curve analysis, run and eluted from a 1% agarose gel and Sanger sequenced (AGRF, Brisbane).

2.6. Total and small RNA sequencing analysis

For processing of total RNA-Seq data we used CLC Genomics Workbench (version 10.1.1) to remove adapter sequences and reads with low-quality scores from datasets. We applied the quality score of 0.05 as the cut-off for trimming. As described in CLC Genomic Workbench manual, the program uses the modified-Mott-trimming algorithm for this purpose. For assembly of the CDS regions of densovirus from Aag2 cells we used the CLC *de novo* assembler with default word length and bubble sizes. Assembled contigs were then queried using BLASTn against the AalDNV-1 strain (Genbank ID: X74945).

For analysis of cytoplasmic and nuclear libraries of both Aag2 and the Aag2.*w*MelPop-CLA small RNA (sRNA) libraries, we used the approach previously described (Mayoral et al., 2014a). For normalization and comparison between sRNA libraries we used reads per million. Unmapped reads less than 16 nt and greater than 32 nt were trimmed from all libraries and sRNAs were then mapped to our assembled contig using the strict mapping criteria (mismatch, insertion and deletion costs: 2:3:3, respectively). For analysis of nucleotide frequency and conservation of AalDNV-1 piRNAs, the RNA-Seq tool on CLC Genomics Workbench was used to sense and antisense strands with default mapping parameters. Mapped reads were then extracted, trimmed to individual nucleotide lengths and visualized using WebLogo (Crooks et al., 2004).

2.7. Phylogenetic analysis

To determine the relatedness between the assembled CDS region of Aag2 densovirus and the previously reported densovirus species of Culicidae mosquitoes, we aligned the CDS regions using the ClustalW algorithm on CLC Genomics Workbench. A maximum likelihood phylogeny (PhyML) was constructed. A hierarchical likelihood ratio test (hLRT) with a confidence level of 0.01 suggested that the General Time Reversible (GTR) +G (Rate variation 4 categories) and +T (topology variation) nucleotide substitution model was the most appropriate. 1000 bootstrap replicates were performed with 95% bootstrap branching support cut-off.

3. Results

3.1. Presence and assembly of Aedes albopictus densovirus (AalDNV-1) genome in Ae. aegypti and Ae. albopictus cells

The *Ae. aegypti* cell line Aag2 (Peleg, 1968) is a robust cell line known to be persistently infected with PCLV (Aguiar et al., 2015; Maringer et al., 2017) as well as CFAV (Cammisa-Parks et al., 1992; Scott et al., 2010). In addition to these viruses, a recent study also assembled a contig with the small RNA fraction of Aag2 cells with high pairwise nucleotide similarity to Aedes aegypti densovirus 2 (AaeDNV-2) (Aguiar et al., 2015). We conducted total RNA sequencing and qPCR analysis to determine the presence and the quantity of densovirus genomes in our Aag2 cells.

After adapter and quality trimming of sequencing data, a total of 93,137,517 clean reads were used for *de novo* assembly of contigs. BLASTn analysis of assembled contigs to the non-redundant nucleotide National Center for Biotechnology Information (NCBI) database revealed a 3937 bp contig identified as 99% identical with highest pairwise nucleotide identity (3680/3721) to Aedes albopictus densovirus (AalDNV-1) (X74945) (Boublik et al., 1994). While this is listed as AalDNV-2 on NCBI, the accepted nomenclature for this densovirus strain is AalDNV-1 (Bergoin and Tijssen, 2010). Assembly was checked by re-mapping to the contig and manually checking for errors. The average coverage of the densovirus contig was 600 × (Fig. 1A). Prediction of open reading frames from this contig showed that it was coding-complete with no premature stop truncations and represents a *bona fide* DNV genome.

As we have assembled a related strain to AalDNV-1, and the original

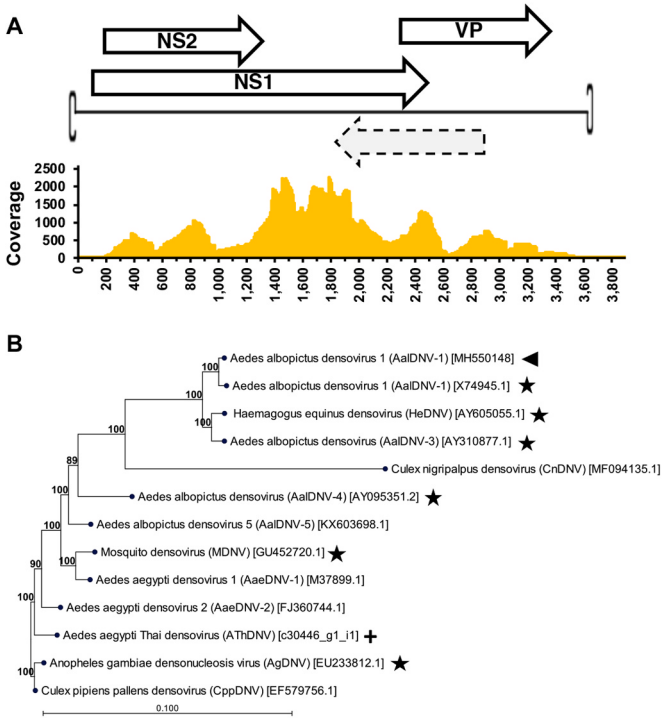

Fig. 1. (A) The schematic diagram and mapping coverage of the genome of Aedes albopictus densovirus (AalDNV-1) assembled from Aag2 cells. (B) Phylogenetic relationship between the AalDNV-1 strain from our Aag2 cells (indicated by an arrowhead) and other densoviruses previously reported in mosquitoes. A star denotes isolation from a mosquito cell line. Maximum likelihood phylogeny (PhyML) between AalDNV-1 strains using a General Time Reversible (GTR) + G +T model with 1000 bootstraps. Branch lengths represent expected numbers of substitutions per nucleotide site. Genbank accession numbers are listed in square brackets. + is available from Supplementary file 1 in (Zakrzewski et al., 2018).

designation of this virus, Aedes parvovirus (AaPV) (Boublik et al., 1994), was harvested from *Ae. albopictus* C6/36 cell lines, and as these viruses are generally named after host species from which the virus was isolated from, it may not represent the true origin of the virus (Carlson et al., 2006). Phylogenetic analysis of this contig was conducted from published and deposited mosquito DNV strains available in the NCBI nr database: AaeDNV-1 (M37899) (Afanasiev et al., 1991), AaeDNV-2 (AY095351.2) (Chen et al., 2004), AalDNV-1 (X74945) (Boublik et al., 1994), AalDNV-3 (AY310877) AalDNV-5 (KX603698.1), MDNV (BR_07) (Mosimann et al., 2011), Haemagogus equinus densovirus (HeDNV) (AY605055.1) (Paterson et al., 2005), and Aedes Thailand densonucleosis virus (AThDNV) (Kittayapong et al., 1999; Roekring et al., 2006; Zakrzewski et al., 2018). Phylogenetic tree rooted to Anopheles gambiae densovirus (AgDNV) EU233812.1 (Ren et al., 2008) and Culex pipiens pallens densovirus (CpDNV) (EF579756.1) (Zhai et al., 2008) showed that the densovirus persistently infecting Aag2 cells was well supported within a clade from densoviruses previously found in Culicinae cell lines (Fig. 1B). The evolutionary rate between the original Aedes parvovirus genome isolated in 1994 from *Ae. albopictus* C6/36 cells (Boublik et al., 1994) and our contig corresponds to $\sim 5 \times 10^{-4}$ subs/site/year. While this is considered a high substitution rate for a DNA virus, and similar to those of RNA viruses (Jenkins et al., 2002), it has been shown that other mammalian parvoviruses such as canine parvovirus have $\sim 10^{-4}$ subs/site/year (Shackelton et al., 2005) and ssDNA viruses have rates of evolution generally reported between the range 10^{-3} and 10^{-5} subs/site/year (Jenkins et al., 2002).

3.2. Higher AalDNV-1 infection is associated with Wolbachia infection in Aedes cells

To test the incidence and abundance of AalDNV-1 in our various *Aedes* cell lines, qPCR was conducted on genomic DNA extracted and purified from *Ae. aegypti* Aag2 cells and different Aag2 derivations: Aag2.*w*MelPop-CLA cells (hereafter Aag2-Pop), and Aag2-Pop cells cleared of *Wolbachia* with tetracycline treatment (hereafter Aag2-PopT). A stably infected Aag2-*w*AlbB line was generated by transinfection of Aag2 cells with the *Wolbachia* *w*AlbB strain from Aa23 cells (O'Neill et al., 1997) as well as a tetracycline cured Aag2-*w*AlbBT. Additionally, the *Ae. aegypti* cell line Aa20 was also tested. We also analysed *Ae. albopictus* cell lines C6/36, Aa23, and its tetracycline cured Aa23-Tet cells. Out of all the cell lines tested, the greatest relative AalDNV-1 copy number relative to host RPS17 was in C6/36 cells ($\bar{x} = 15{,}633$ n = 3) (Fig. 2A). This cell line has been demonstrated to be Dicer-2 deficient and hence it produces high titers of arboviruses compared with Dicer-2 proficient cell lines (Brackney et al., 2010). Considering the Aag2 cell line and its derivatives, there was statistically significantly less AalDNV-1 genome copies in both Aag2 ($\bar{x} = 207.33$, n = 3) and Aag2-PopT ($\bar{x} = 223$, n = 3) cells when compared with Aag2-Pop cells ($\bar{x} = 5943$, n = 3) ($p \leq 0.01$; Student's *t*-Test). Similarly, Aag2-*w*AlbB cells had a higher abundance of AalDNV-1 copy numbers ($\bar{x} = 877$, n = 3) compared with tetracycline cured Aag2-*w*AlbT ($\bar{x} = 412$, n = 3) and also the Aag2 cells ($p \leq 0.05$; Student's *t*-Test). A similar trend was also observed for AalDNV-1 copy number in Aa23 ($\bar{x} = 0.258$, n = 3) cells and their tetracycline-cured line Aa23-T cells ($\bar{x} = 0.0684$, n = 3) ($p \leq 0.05$; Student's *t*-Test) (Fig. 2A).

We could not amplify any AalDNV-1 from the Aa20 cell line. As such, we used this cell line as a means to find out if the AalDNV-1 particles from both C6/36 and Aag2 cells were infectious. Purified supernatant from both C6/36 (Fig. 2B) and Aag2 medium (data not shown) were shown to increase over a 5-day time course, with Aa20 cells showing high permissibility to infection but no obvious cytopathic effect.

3.3. AalDNV-1 infection is enhanced by Wolbachia in a density-dependent manner in Ae. aegypti and Ae. albopictus cells

To determine the relative density of *Wolbachia* in the aforementioned cells, we conducted qPCR validating the presence of high *Wolbachia* genome copies in Aag2-Pop ($\bar{x} = 18.9$, n = 3), Aag2-*w*AlbB ($\bar{x} = 0.69$, n = 3) and Aa23 ($\bar{x} = 0.21$, n = 3) cells compared with their tetracycline-cured lines (Fig. 3A). To further explore the association between *Wolbachia* presence and higher genome copies of AalDNV-1 in *Aedes* cells, we generated 32 DNA samples from ten successive tetracycline (5 μ g/mL) treatments of Aag2-Pop cells and plotted the relationship between density of *Wolbachia* genome copies over genome copies of AalDNV-1. Linear regression analysis showed there was a positive relationship between *Wolbachia* genome copies in these cells ($R^2 = 0.5647$; $p \leq 0.0001$) (Fig. 3B). This trend was also observed when cross-checking 28 historical samples from 2017 from nine successive tetracycline (5 μg/mL) treatments in the production of the Aag2-Pop-T line (Fig. S1) ($R^2 = 0.6784$; $p \leq 0.0001$). In addition to tetracycline treatment of Aag2-Pop cells, the stably infected Aag2-*w*AlbB line was monitored every two passages over 30 passages for *Wolbachia* density and AalDNV-1 copy number (n = 15). Linear regression analysis showed there was also a positive relationship between *Wolbachia* density ($R^2 = 0.6779$; $p \leq 0.001$) and AalDNV-1 genome copy number in these cells (Fig. 3C). Taken together, *Wolbachia* appears to enhance AalDNV-1 replication and this enhancement is in a density-dependent manner.

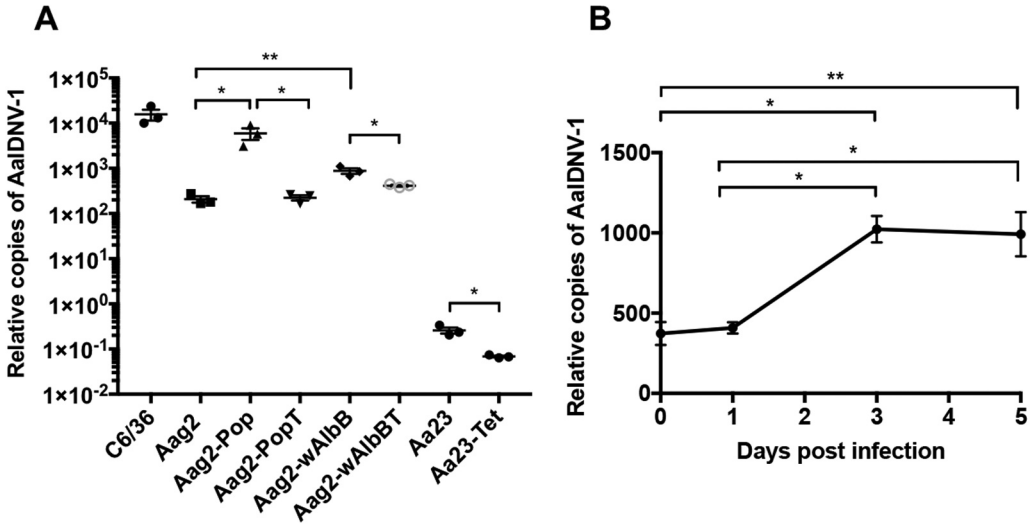

Fig. 2. *Ae. aegypti* Aag2 and *Ae. albopictus* Aa23 cells and their derivatives and *Ae. albopictus* C6/36 cells are infected with AalDNV-1 with virus density associated with *Wolbachia* infection. (A) AalDNV-1 levels quantified with qPCR analysis using genomic DNA extracted from Aag2 and Aag2-Pop, cells treated with tetracycline Aag2-PopT, an uninfected control *Ae. aegypti* cell line Aa20 and in *Ae. albopictus* Aa23 cells stably infected with wAlbB. *RPS17* gene was used as a normalizing reference. (B) AalDNV-1 particles are infectious. Aa20 cells that lack AalDNV-1 were inoculated with medium from C6/36 cells and collected for DNA extraction at 0, 1, 3 and 5 days post-inoculation. Virus DNA levels, quantified by qPCR, increased over time. * $p \leq 0.05$, ** $p \leq 0.01$.

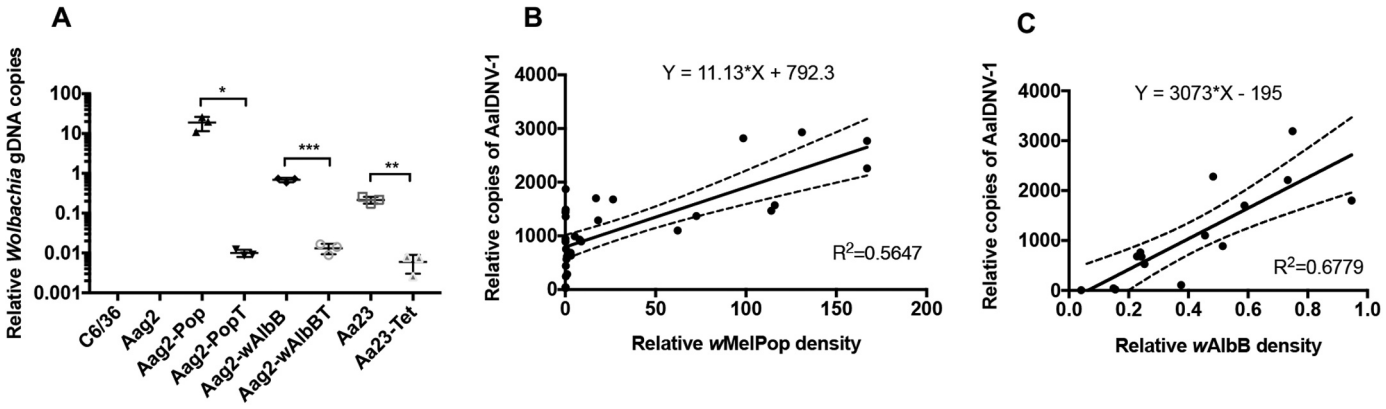

Fig. 3. *Wolbachia* enhances AalDNV-1 infection in a density-dependent manner. (A) Density of *Wolbachia* in cell lines determined by qPCR using the *wsp* gene relative to the host *RPS17* gene. (B) Linear regression analysis of AalDNV-1 genome copies over *Wolbachia* genome copies in Aag2 cells stably infected with *w*MelPop-CLA and sequentially cleared of *Wolbachia* through tetracycline treatment. (C) Aag2 cells transinfected with *w*AlbB over 30 passages. * $p \leq 0.05$; ** $p \leq 0.01$; *** $p \leq 0.001$.

3.4. AalDNV-1 gene transcripts are targeted by the RNAi response

RNAi response is observed in mosquitoes against disparate RNA virus infections. This response includes the microRNA (miRNA) pathway (20–24nt), small interfering RNA (siRNA) pathway (21nt), and the exogenous PIWI-interacting RNAs (piRNA) (25–30 nt) (Blair and Olson, 2015; Hussain et al., 2016; Schnettler et al., 2013). Transcripts of DNA virus genes have been demonstrated to be targeted and modulated by the RNAi pathway in diverse insect DNA virus interactions (Bronkhorst et al., 2012; Jayachandran et al., 2012b; Sabin et al., 2013).

To explore the RNAi response to densoviruses in Aag2 and Aag2-Pop cells, the small RNA portion of nuclear and cytoplasmic fractions of Aag2 and Aag2-Pop cells previously sequenced (Mayoral et al., 2014a, 2014b) was adapter trimmed, pooled and mapped to the assembled AalDNV-1 contig. Analysis of pooled libraries of Aag2 and Aag2-Pop cells revealed there was not much difference between the number of 18–32nt reads that were derived from AalDNV-1 in Aag2 (n = 28,99; 0.34%) and Aag2-Pop (n = 52,693; 0.33%) cells after normalization of libraries. In both Aag2 and Aag2-Pop cells, more sRNA reads mapped to the genome of AalDNV-1 (Aag2: 87.45%, Aag2-Pop:80.91%) compared to the antigenome of AalDNV-1 (Aag2: 12.54%, Aag2-Pop: 19.08%). The higher proportion of reads mapping to the genome of AalDNV-1 in Aag2 cells is similar to the 7:1 genome: antigenome ratio previously reported in *Culex pipiens molestus* mosquitoes infected with Mosquito densovirus (MDNV) (Mosimann et al., 2011).

Additionally, the patterns of regions of virus-derived small RNAs mapping to the AalDNV-1 viral genome were the same between both Aag2 (Fig. 4A) and Aag2-Pop cells (Fig. 4B). Total sRNA reads mapped unevenly throughout the AalDNV-1 genome with “hot spot” regions being highly targeted (regions 400–570nt and 2300–2800nt). In the RNAi response, 21 nt reads are indicative of virus-derived short interfering RNAs (vsiRNAs). These vsiRNAs are generated by the cleavage of viral dsRNA by the RNase III enzyme Dicer-2 (Sabin et al., 2013). Considering AalDNV-1-derived vsiRNAs across all the four individual libraries, there was a higher abundance of 21 nt vsiRNAs in Aag2-Pop cells (21.18% in the nuclear fraction and 19.53% in the cytoplasmic fraction) compared with those in the Aag2 libraries (15.28% of the nuclear library and 14.89% of the cytoplasmic sRNA library) (Fig. 4C-D). Individual cytoplasmic and nuclear mapping profiles for all libraries are available in Fig. S2. This result shows that *Wolbachia* infection of Aag2 cells results in a higher absolute abundance of AalDNV-1-derived vsiRNAs, which is consistent with the qPCR data (Figs. 2 and 3) that suggested higher replication of AalDNV-1 in the presence of *Wolbachia*. It is important to note that these results should not be used to interpret that there is a greater efficiency of vsiRNA production in *Wolbachia*-infected cells. It seems reasonable to suggest that the higher abundance of vsiRNAs produced in *Wolbachia*-infected cells could be as a result of greater transcriptional activity of AalDNV-1 due to *Wolbachia* infection.

While densoviruses do not use dsRNA as a replicative intermediate, it has been previously reported that parvoviruses produce dsRNA (Son et al., 2015; Weber et al., 2006). To further examine the biogenesis of the vsiRNAs in ssDNA virus infection, we trimmed all libraries to 21 nt fractions and re-mapped the reads to the AalDNV-1 genome (Fig. 5A-B). With the exception of high “hot spot” coverage of the genome strand by the sRNAs, we noticed a pattern of “mirroring” of vsiRNA between genome position ~400–3000 nt which corresponds to the *NS1/NS2* transcription and the beginning of the *VP* gene. This pattern of mapped reads has been shown in *Drosophila* cells infected with vaccinia virus (VACV, *Orthopoxvirus*) and is due to overlapping transcription of genes on both strands of the DNA virus genome (Sabin et al., 2013). This suggests that the biogenesis of these vsiRNAs may be derived through overlapping transcription of genes on the genome and antigenome strands.

3.5. Production of AalDNV-1 derived PIWI-interacting RNAs in Aedes cells

In addition to vsiRNAs, another class of sRNAs has been demonstrated to be produced in response to virus replication called P-element-induced Wimpy testis gene (PIWI)-interacting RNAs (piRNAs). During virus replication, single-stranded RNA is enzymatically cleaved into 25–29 nt fragments that bind to PIWI or Argonaute (Ago) proteins. These virus-derived piRNAs (vpiRNAs) are produced in somatic tissues against RNA virus infections in *Ae. aegypti* and *Ae. albopictus* (Morazzani et al., 2012; Wang et al., 2018). Primary piRNAs bound to PIWI proteins have been shown to have a sequence bias for uridine at the first position (U_1). By comparison, Ago-3 associated secondary piRNAs have been shown to have a bias for adenine at position ten (A_{10}). PIWI and Ago proteins have been demonstrated to have 10 nt of overlapping complementary bases (U_1 - A_{10})(Vodovar et al., 2012). This is broadly referred to the “ping-pong” signature of piRNAs.

In an RNAi screen of *Ae. aegypti* cells infected with Sindbis virus (SINV, *Togaviridae*), Piwi5 was identified to associate with primary vpiRNAs, whereas Ago3 was demonstrated to bind to secondary vpiRNAs (Miesen et al., 2015). Depletion of Piwi5 and Ago3 proteins in *Aedes* cells resulted in a drastic depletion of piRNAs against SINV; however, this did not translate into a change in virus replication (Miesen et al., 2016a).

While it has been previously reported that 25–29 nt sRNA reads were present in *C. pipiens molestus* mosquitoes infected with MDNV (Mosimann et al., 2011), the vpiRNA signature of these 25–29 nt reads were not examined for the presence of primary and secondary piRNAs. As there has been no previous examination of vpiRNAs in the case of DNA viruses of insects, we examined the mapping pattern and also the

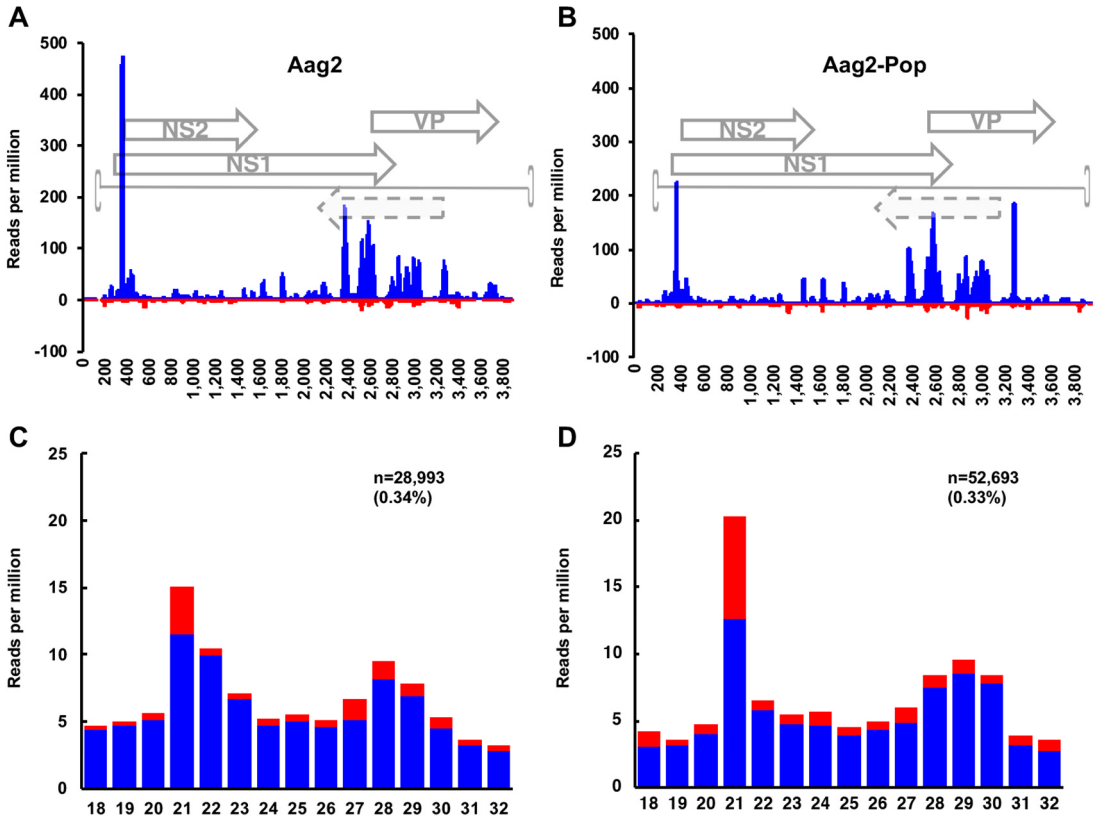

Fig. 4. Profile of total normalized 18–32nt reads mapped to the genome strand (blue) and antigenome strand (red) of AalDNV-1 in combined nuclear and cytoplasmic libraries of (A) Aag2 cells (A) and (B) Aag2-Pop cells. Composition and profile of virus-derived small RNA reads mapped to AalDNV-1 in (C) Aag2 and (D) Aag2-Pop cells.

"ping-pong" signature of AalDNV-1-derived 25–29 nt reads in both Aag2 and Aag2-Pop cells. In comparison to the vsiRNA profile, the vpiRNAs were most abundantly targeted towards the end of the *NS2* and *VP* genes (Fig. 6A-B). It also appears that there are no clear differences between the profile and mapping of vpiRNAs between Aag2 and Aag2-Pop cells suggesting that *Wolbachia* may have no effect on the piRNA pathway *in vitro*. There were also far more vpiRNAs targeting the AalDNV-1 genome in both the pooled datasets (Fig. 4A-B) and individual cytoplasmic and nuclear fractions compared with the antigenome (Fig. S2).

In the pooled nuclear and cytoplasmic libraries for both Aag2 and Aag2-Pop cells, there was a typical "ping-pong" signature (U_1 - A_{10}) of secondary piRNAs in vpiRNAs in all 25–29 nt sRNAs. However, when we considered just the cytoplasmic and the nuclear fractions of the Aag2 and Aag2-Pop cells individually, we noticed that there was exclusive production of primary piRNAs (U_1 biased) targeted against the negative-sense strand and no bias towards an A_{10} signature in the nuclear fraction of both Aag2 and Aag2-Pop cells (Fig. 6C). In contrast, a typical "ping-pong" signature (U_1 - A_{10}) was observed in reads from the cytoplasmic fraction (Fig. 6D).

3.6. A defective AalDNV-1 genome exists in published DNA, RNA and sRNA Aag2 datasets and exclusively produces vsiRNAs

The *Ae. aegypti* Aag2 cell line is a heterogenous embryonic cell line (Peleg, 1968) ubiquitous in arbovirus research laboratories for its robust immune response (Barletta et al., 2012). The Aag2 cell line was recently sequenced through long-read Pac-Bio assembly (Whitfield et al., 2017). To determine if AalDNV-1 was present in the assembly, we scanned the assembled contigs for the presence of AalDNV-1. One 80 kb

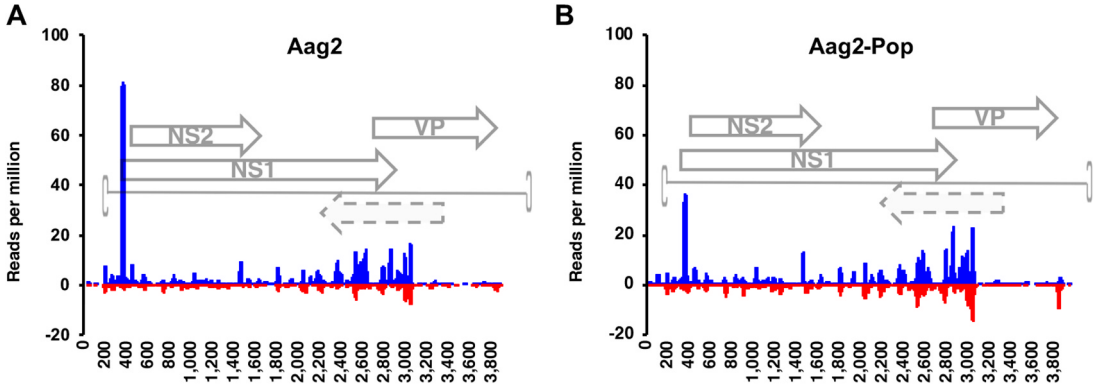

Fig. 5. The host RNAi response to AalDNV-1. Mapping profile of the 21nt virus-derived siRNAs (vsiRNAs) targeting AalDNV-1 in (A) Aag2 and (B) Aag2-Pop cells.

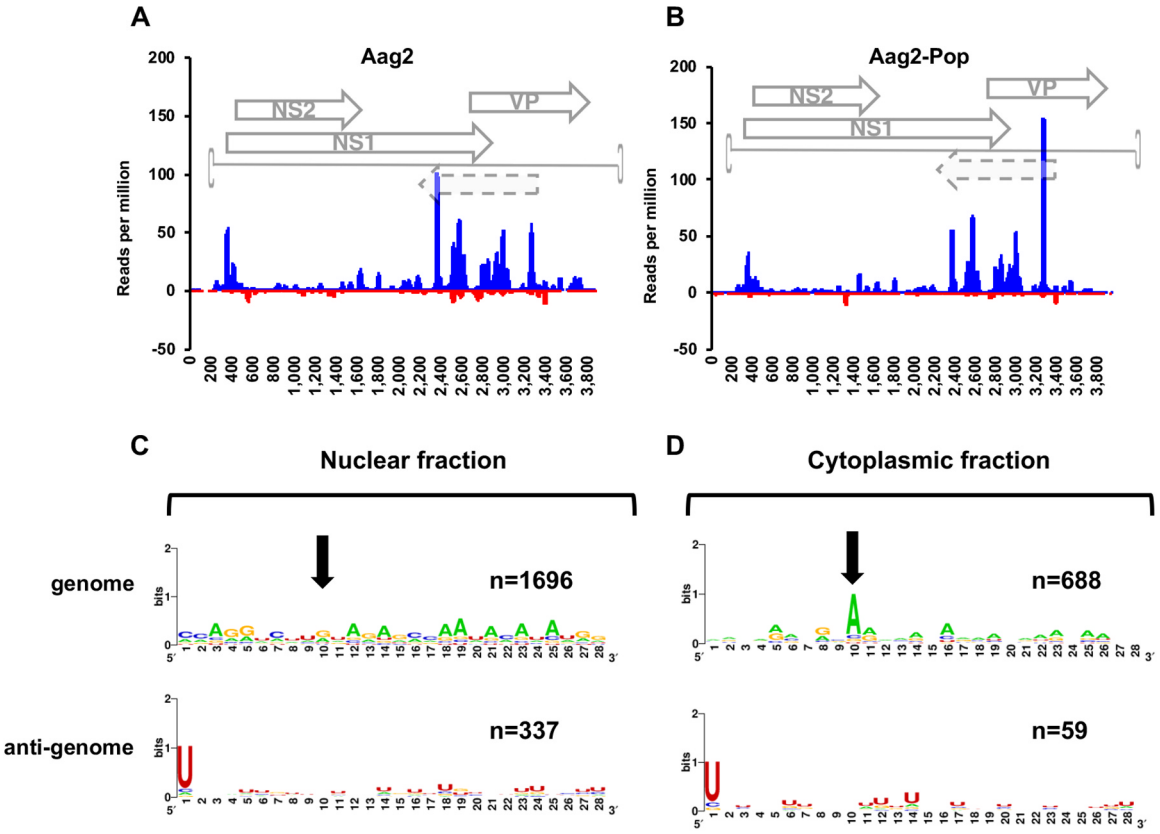

Fig. 6. The host piRNA response to AalDNV-1. Mapping profile of 25–29nt virus-derived PIWI-interacting piRNAs (vpiRNA) to AalDNV-1 in (A) Aag2 and (B) Aag2-Pop cells. Relative nucleotide frequency and conservation per 28nt vpiRNAs mapped to the AalDNV-1 genome and antigenome in (C) the nuclear and (D) the cytoplasmic fractions of Aag2 cells. Arrow denotes A_{10} position absent in the nuclear fraction. Only Aag2 28nt has been shown as a representative.

contig (2140) showed a number of hits to our assembled AalDNV-1 genome (Fig. 7A). Interestingly, it appeared that the contig was assembled in the sense and then antisense orientation for ~80 kb. Due to the nature of the movie-length PacBIO SMRT Sequencing, if the polymerase runs to the end of the insert, it will continue looping back on the template molecule until the acquisition period ends (Eid et al., 2009). Analysis of the raw data indicated that this was the case as the forward and reverse of the genome were shown immediately in the raw data. Further analysis of the contig showed that it was a partial AalDNV-1 genome assembled by itself, but the *VP* gene of the genome was disrupted while the terminal hairpins and *NS1/2* genes remained intact (Fig. 7B).

The Aag2 cell line is RNAi proficient and numerous studies have used the cell line to elucidate components of the siRNA and the piRNA pathways in virus-host interactions. We were interested to re-analyse this collective resource to look at determinants of the RNAi response in Aag2-densovirus interactions. We downloaded RNA sequencing data from a recent study characterising the role of the PIWI protein 4 in the antiviral pathway (Varjak et al., 2017). Mapping sRNA reads to our assembled reference contig from the parental Aag2 cell line (AF5), we noticed there was also an absence of mapped reads to the *VP* region of the densovirus genome (Fig. 7B). This was not due to sequencing depth as AalDNV-1 reads comprised as many as 1.08% of the total reads (n = 122,398). In addition to this absence of mapped reads towards the *VP* gene region, we noticed that vpiRNAs were absent and not produced against this contig (Fig. 7D). Greater than 80% of the mapped reads are 21 nt in size and mapped equally to the genome and antigenome, without the 7:1 genome:antigenome strand bias presented here and previously in mosquitoes infected with DNVs (Mosimann et al., 2011).

We expanded our search to other Aag2 datasets deposited in the Short Read Archive on NCBI. Subsequent re-mapping of sRNA reads from Aag2 cells indicated that this portion of AalDNV-1 was "silent" or potentially defective in every Aag2 dataset except the total RNA and sRNA data produced from sequencing data from our Aag2 cells. Parvoviruses in mammals have been shown to generate defective particles during high-multiplicity infections (Faust and Ward, 1979). The genome of these defective particles varied in size but always retained the terminal palindromes. We suspected that the AalDNV-1 densoviruses common in Aag2 cells may exist as a defective interfering genome. We designed a PCR primer set that encompassed the region which appeared to be absent in other Aag2 data and were able to amplify an appropriately-sized amplicon in our Aag2 cells (data not shown).

In addition to the parental Aag2 (AF5) line, sRNA data from a second Dicer-2 knockout (KO) cell line (AF319) was available for analysis. Reads from the Dicer-2 KO were mapped against our AalDNV-1 reference contig. Once again, there were an absence of reads mapping to the suggested truncated region with only 2485 reads representing 0.01% of the library (Fig. 7C). In addition, 21 nt vsiRNAs were almost absent against AalDNV-1 in Dicer-2 KO AF319 cells while the vpiRNAs increased (Fig. 7D). This finding agrees with previous studies in *Aedes* cell lines showing that in the absence of an efficient siRNA response, more piRNA-size sRNAs are produced against RNA virus infection (Brackney et al., 2010; Scott et al., 2010).

As disruption of the *VP* gene results in lack of productive AalDNV-1 virion production, and that *Ae. aegypti* flanking sequences are absent in the assembled contig from the Aag2 cells used for genome sequencing, the defective AalDNV-1 genome should not be integrated into the host genome, but extrachromosomally maintained.

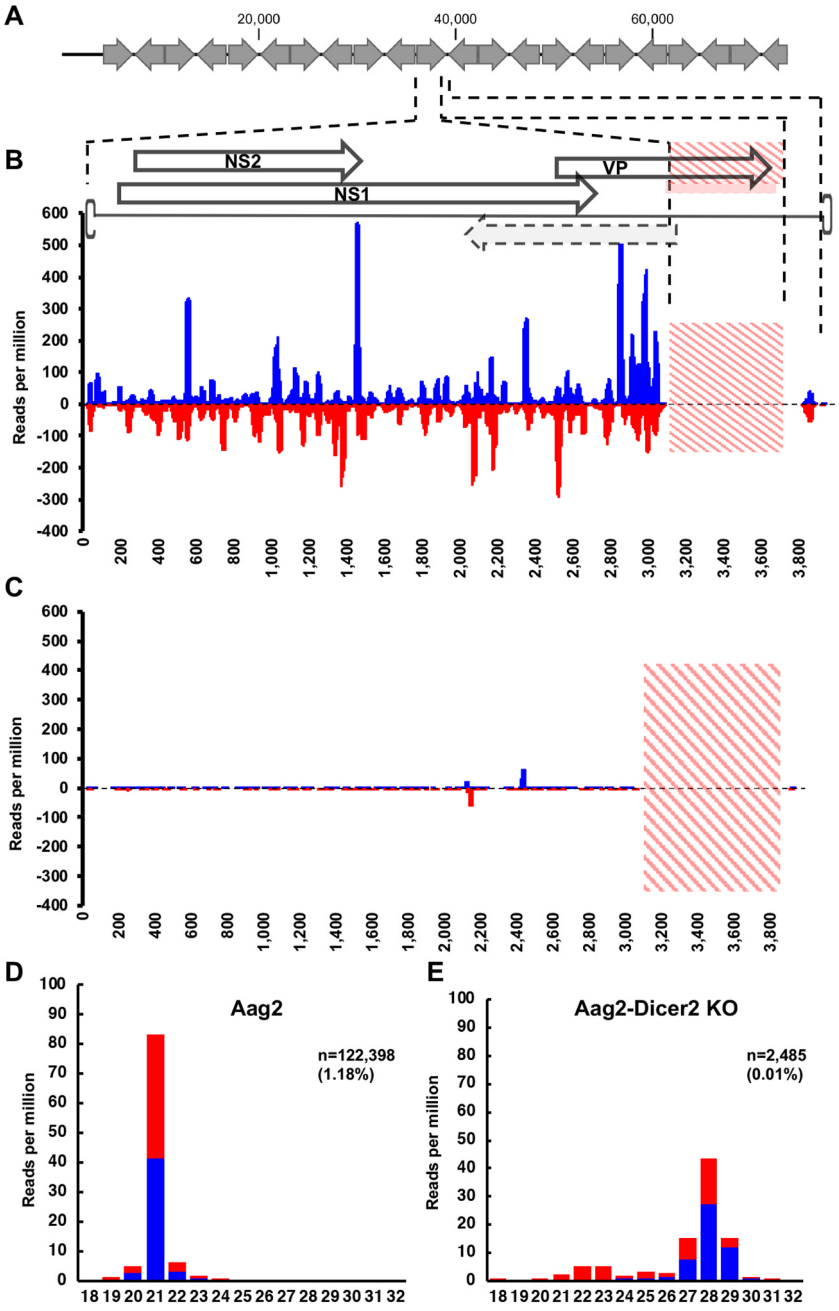

Fig. 7. A defective AalDNV-1 particle exists in other Aag2 cells and is targeted almost exclusively by the vsiRNA pathway. (A) Contig 2140 from the Aag2 cell line genome project. Arrows denote orientation of the genome. Mapped 18–32nt reads to the AalDNV-1 genome in (B) the parental Aag2 cell line (AF5) and (C) the Dicer-2 knockout Aag2 cells (AF319). Size distribution of mapped sRNA reads from (D) the parental Aag2 cell line (AF5), and E) Dicer-2 knockout (AF319) Aag2 cell line. Red dashed portions in (B) and (C) denote the absence of mapped reads to the virus genome.

4. Discussion

4.1. Wolbachia-DNA virus interactions

Complex interactions between the endosymbiont *Wolbachia* and its insect host often contribute to modulation of virus titer within the insect. Much of what we currently understand about *Wolbachia*-virus interactions has been characterised using *Drosophila-Wolbachia* models and single-stranded positive-sense RNA viruses. For example, in *Drosophila simulans* challenged with Flock House virus (FHV, *Nodaviridae*) and Drosophila C virus (DCV, *Dicistroviridae*), it was determined that *Wolbachia* was responsible for 93.6% and 70.9% of variance in viral titer, respectively. Further, it was demonstrated that *Wolbachia* density accounted for 86% of *Wolbachia*-mediated protection within the host (Martinez et al., 2017). This density-dependent refractoriness to RNA virus infection conferred by *Wolbachia* has been demonstrated in a number of *in vivo* and *in vitro* studies (Lu et al., 2012; Martinez et al., 2014; Osborne et al., 2012). In *Ae. albopictus* mosquitoes infected with *w*AlbB, clearance of *w*AlbB *in vivo* had no effect on the transmission of DENV or CHIKV but was shown in cells to restrict DENV in a density-dependent manner (Lu et al., 2012). Here, we show that instead of *Wolbachia*-mediated virus refractoriness, in the presence of *Wolbachia* there is a density-dependent enhancement of a ssDNA virus.

One potential explanation for *Wolbachia*-mediated DNA virus enhancement is in the interplay between reactive oxygen species (ROS) and DNA repair. Increased oxidative stress in various arthropod hosts as

a consequence of *Wolbachia* infection is fairly well-reported (Brennan et al., 2012; Wong et al., 2015). It is thought that *Wolbachia*-containing vacuoles located in the host cell cytoplasm may introduce greater oxidative stress through the higher production of ROS. Disruption of the redox homeostasis in *Ae. albopictus* Aa23 cells has been shown to increase the incidence of ROS-induced DNA damage as demonstrated by increased base 8-oxo-deoxyguanosine in these cells (Brennan et al., 2012). Densoviruses replicate exclusively in the nucleus and require DNA polymerase host machinery for replication. Densoviruses and parvoviruses have also been demonstrated to broadly trigger and require the DNA damage response (DDR) to recruit DNA polymerase cofactors machinery for productive DNA replication (Hristov et al., 2010). It may therefore be possible that the mechanism of *Wolbachia*-mediated DNA virus enhancement lies in the association between ROS induction and the subsequent activation of the DNA damage response (DDR) in *Aedes* cells.

The results reported here expand upon previous findings of *Wolbachia*-DNA virus interactions in other systems and suggest that both *w*MelPop-CLA, which is a supergroup A *Wolbachia* strain, and *w*AlbB, which is a supergroup B *Wolbachia* strain, can enhance replication of densovirus. As a consequence of this density-dependent enhancement of DNA virus replication in insect hosts, it would be advantageous for *Wolbachia* titers to be low enough to have limited effect on the host. *Wolbachia* density has been consistently demonstrated to be significantly lower in the somatic tissues when compared to testes and ovaries of *Drosophila, Ae. albopictus* and transinfected *Ae. aegypti* (Lu et al., 2012; Osborne et al., 2012). Additionally, it has been shown in the transinfected *Ae. aegypti* WB1 strain, *Wolbachia* density is significantly lower in the *Ae. albopictus* HOU strain than in the transinfected *Ae. aegypti* (Lu et al., 2012). We observed a similar trend in our *Ae. aegypti* cells infected with *w*AlbB. The *Ae. aegypti* transinfected cells had a *Wolbachia* density as high as 3-fold more than Aa23 cells. How these *in vitro* findings may translate into potential pathological consequences in *Wolbachia*-infected *Ae. aegypti* mosquitoes requires further analysis. Currently, we have a limited scope as to the diversity and incidences of DNA viruses of *Ae. aegypti* and *Ae. albopictus* mosquitoes. Even in the most widely studied AalDNV-1 and AaeDNV strains little information on the ecology of these viruses is known. In one report of wild populations of *Ae. aegypti* in Thailand, infections with Thai strain densovirus (AThDNV) were demonstrated to be as high as 44% (Kittayapong et al., 1999). Experiments with Invertebrate Iridescent virus type 3 (IIV-3, *Chloriridovirus*) in *Ae. aegypti* and *Ae. albopictus* cells suggest that cells from both mosquitoes are permissive to infection (Becnel and Pridgeon, 2011). It has also been demonstrated that laboratory colonies of *Ae. aegypti* can be experimentally infected with Invertebrate iridescent virus 6 (IIV-6, *Iridoviridae*) (Marina et al., 1999, 2003). It may be possible that large scale release of *Wolbachia*-infected mosquitoes together with MDNVs could synergistically improve the efficiency of these programs, as has been a recommendation for the improvement of Sterile Insect Technique release programs (Bouyer et al., 2016; Bouyer and Lefrançois, 2014).

4.2. Host RNAi response to densovirus

RNAi response, in particular the siRNA pathway, is a powerful antiviral response against RNA viruses in insects due to the nature of the genome and production of dsRNA intermediates during replication. However, experimental evidence has also shown that the siRNA response is exerted by insects towards dsDNA viruses (Bronkhorst et al., 2012; Jayachandran et al., 2012a; Karamipour et al., 2018; Kemp et al., 2013), most likely against overlapping RNA transcripts produced during transcription of the viral genome. Our results showed that the host siRNA response could also be triggered by a ssDNA virus. In both the nuclear and cytoplasmic fractions of Aag2-Pop cells there was a greater absolute abundance of 21 nt vsiRNAs mapping to the AalDNV-1 genome, which correlates with higher replication of the virus in the cells. While it has been previously demonstrated that *Wolbachia* *w*MelPop-CLA interferes with the localisation of Argonaute-1 within *Ae. aegypti* infected cells, there was no evidence for manipulation of the abundance or localisation of Argonaute-2 when analysed at the protein level (Hussain et al., 2013b). A recent report showed that in *w*Mel infected Aag2 cells Argonaute-2 transcript levels are significantly upregulated (Terradas et al., 2017) and may contribute in a small way towards *Wolbachia*-mediated blocking of DENV-2 in these cells by enhancing RNAi. However, we believe a more likely reason for the increased vsiRNA production against AalDNV-1 in the presence of *Wolbachia* could be the greater abundance of dsRNAs produced by overlapping transcripts due to enhanced replication of the virus.

In addition to demonstrating that vsiRNAs are produced against AalDNV-1 in *Aedes* cells, we have also revealed an interesting aspect of the RNAi response to DNA viruses, which is the production of 25–29 nt vpiRNAs, that has been shown when insect cells become infected with a number of RNA viruses (Reviewed in Miesen et al., 2016b). We show for the first time that vpiRNAs could also be produced against DNA viruses. A large number of vpiRNAs were found in AalDNV-1 infected Aag2 cells mostly towards the end of the genome. Furthermore, these vpiRNAs displayed the characteristic “ping-pong” signature (U_1 - A_{10}), with the A_{10} signature being predominantly found in vpiRNAs in the cytoplasmic fraction. The proteins Piwi5 and Ago3 are the core proteins of the mosquito ping-pong loop and occur almost exclusively in the cytoplasm (Miesen et al., 2015). As the replication of densoviruses are exclusively nuclear, it may be the case that the biogenesis of the primary U_1 piRNAs in the nucleus may not be from Ago3/Piwi5 cleavage but may in fact be targeted by Zucchini (Zuc).

As the replication of Aedes albopictus densovirus occurs exclusively in the nucleus, transcripts of genes may be targeted and processed into functional miRNAs from the host Dicer-1 machinery as is reported in other DNA viruses (Hussain and Asgari, 2010; Hussain et al., 2008). As per the previous report of manipulation of the Argonaute-1 protein by *Wolbachia* in *Aedes* cells, it still remains to be elucidated if functional miRNAs are produced by AalDNV-1 and if this is modulated by *Wolbachia* infection.

4.3. Has the AalDNV-1 defective genome cleared AalDNV-1 from most Aag2 cells?

There has been considerable interest in virus-derived DNA (vDNA) intermediates produced in mosquitoes in response to RNA virus infection (Goic et al., 2016). Work conducted by Poirier and colleagues showed that defective viral genomes (DVGs) form chimeric forms with host LTR retrotransposases to produce circular vDNA (Poirier et al., 2018). These circular vDNA chimeras were then shown to serve to amplify siRNA-mediated antiviral immunity in insects, as mapping profiles indicated that they exclusively produced vsiRNAs (Poirier et al., 2018). Densoviruses are ssDNA viruses until they infect the host. Upon entry into the nucleus, the ssDNA template is “repaired” into a closed circular form. All evidence presented here indicate that the most common and predominant AalDNV-1 in published Aag2 datasets exists as truncated and defective, as it has been demonstrated that plasmids that have disrupted *VP* genes do replicate and express, but they do not produce virions, and need a “helper” virus with a complete *VP* gene (Afanasiev et al., 1999). The defective AalDNV-1 genome produces equal genome and antigenome vsiRNAs. In contrast, in the only other report of RNAi response to DNV infection (Mosimann et al., 2011), there was a 7:1 genome:antigenome bias which is consistent with our data with a prolific AalDNV-1 replication. The viral profile presented here in other Aag2 cells appears to mirror the exact same profile of the RNAi response that was demonstrated in response to defective vDNA virus genomes as demonstrated previously (Poirier et al., 2018). Also, it seems unlikely that the vDNA was produced from the canonical LTR retrotransposase chimerisation events, which has been suggested previously in RNA virus infection (Poirier et al., 2018) and is more likely to

be produced through errant DNA genome production.

In Dicer-2 knockout Aag2 cells, the 21 nt vsiRNAs effectively disappeared, but there was an increase in the number of piRNA size sRNAs against the defective genome. Previous research has shown that in the absence of an efficient siRNA response, more piRNA-size sRNAs are produced against viruses (Brackney et al., 2010; Scott et al., 2010). However, the number of vpiRNAs produced in Dicer-2 knockout cells is far less than those found in our Aag2 cells. Previous work in *Drosophila* suggested that production of piRNAs against nuclear gene transcripts is controlled by a 100 nt *cis*-regulatory element that triggers piRNA production (Ishizu et al., 2015). The vpiRNAs that are produced in response to AalDNV-1 infection in our non-defective Aag2 cell line are targeted towards the end of the *NS2* and *VP* genes. As the *VP* gene is truncated in the defective genome, it may be the case that the lack of vpiRNA production is reduced by the absence of a *cis*-regulatory element within the genome.

Amazingly, it appears that this defective genome has managed to predominate in all published Aag2 datasets. The fixation of this defective genome within common Aag2 cells indicates that the vsiRNAs produced from this viral DNA segment might have been able to successfully clear the non-defective forms. This suggests that vDNA forms of ssDNA viruses may also work to promote tolerance within mosquitoes to DNA virus infections, as is suggested in RNA virus infection. However, this needs to be experimentally explored.

5. Conclusions

In this study, we demonstrate that there are greater levels of AalDNV-1 in the presence of *Wolbachia* in *Aedes* cells. Additionally, this effect is density-dependent and can be induced by both supergroup A and supergroup B *Wolbachia* strains. Further, we revealed that abundant siRNA and piRNA responses are elicited against AalDNV-1. It has been demonstrated that *Ae. aegypti* cells infected with different strains of mosquito densoviruses display different pathologies, with some inducing cytopathic effect and spontaneous induction of apoptosis (Paterson et al., 2005). As the level of densovirus infection significantly increases in the presence of *Wolbachia,* it may be the case that *Wolbachia*-infected *Aedes* mosquitoes could be more sensitive to DNV pathological effects in the environment. Work presented here also suggests that there is a heterogeneity between laboratory Aag2 cells in regard to the presence of complete or defective AalDNV genomes.

As we have demonstrated that *Wolbachia* enhances replication of AalDNV-1 *in vitro*, it seems reasonable to suggest that dual *Wolbachia*-DNV biocontrol strategies may be feasible. However, extensive laboratory and field testing would have to be carried out. At the very least, these strategies do not seem to be incompatible with one another, and may likely work synergistically.

Acknowledgements

The authors would like to acknowledge Dr. Karyn Johnson and Hugo Perdomo Contreras for their valuable insight and discussions. Erica Ward for proofreading and suggestions for improving the structure of the document. We thank Dr. Gareth Price and Dr. Igor Makunin from the University of Queensland for interpretation of the PacBIO sequencing analysis. Additionally, we want to thank the two anonymous reviewers for suggestions on improving the manuscript. Funding: This project was funded by the Australian Research Council (grant number DP150101782) to SA and a University of Queensland scholarship to RP.

Data accessibility accession numbers

The assembled Aedes albopictus densovirus 1 Aag2 strain (AalDNV-1) contig has been deposited in the National Center for Biotechnology Information (NCBI) database under accession number MH550148. Small RNA sequencing data used in this paper is also accessible through GEO series accession number GSE55210.

Appendix A. Supporting information

Supplementary data associated with this article can be found in the online version at doi:10.1016/j.virol.2018.12.006.

References

Afanasiev, B.N., Galyov, E.E., Buchatsky, L.P., Kozlov, Y.V., 1991. Nucleotide sequence and genomic organization of Aedes densonucleosis virus. Virology 185, 323–336.
Afanasiev, B.N., Ward, T.W., Beaty, B.J., Carlson, J.O., 1999. Transduction of *Aedes aegypti* mosquitoes with vectors derived from Aedes densovirus. Virology 257, 62–72.
Aguiar, E.R., Olmo, R.P., Paro, S., Ferreira, F.V., de Faria, I.J., Todjro, Y.M., Lobo, F.P., Kroon, E.G., Meignin, C., Gatherer, D., Imler, J.L., Marques, J.T., 2015. Sequence-independent characterization of viruses based on the pattern of viral small RNAs produced by the host. Nucleic Acids Res. 43, 6191–6206.
Aliota, M.T., Peinado, S.A., Velez, I.D., Osorio, J.E., 2016a. The *w*Mel strain of *Wolbachia* reduces transmission of Zika virus by *Aedes aegypti*. Sci. Rep. 6, 28792.
Aliota, M.T., Walker, E.C., Uribe Yepes, A., Velez, I.D., Christensen, B.M., Osorio, J.E., 2016b. The *w*Mel strain of *Wolbachia* reduces transmission of Chikungunya virus in *Aedes aegypti*. PLoS Negl. Trop. Dis. 10, e0004677.
Ant, T.H., Herd, C.S., Geoghegan, V., Hoffmann, A.A., Sinkins, S.P., 2018. The *Wolbachia* strain *w*Au provides highly efficient virus transmission blocking in *Aedes aegypti*. PLoS Pathog. 14, e1006815.
Asad, S., Parry, R., Asgari, S., 2018. Upregulation of *Aedes aegypti* Vago1 by *Wolbachia* and its effect on dengue virus replication. Insect Biochem. Mol. Biol. 92, 45–52.
Barletta, A.B.F., Silva, M.C.L.N., Sorgine, M.H.F., 2012. Validation of *Aedes aegypti* Aag-2 cells as a model for insect immune studies. Parasites Vectors 5, 148.
Barreau, C., Jousset, F.X., Bergoin, M., 1996. Pathogenicity of the *Aedes albopictus* parvovirus (AaPV), a denso-like virus, for *Aedes aegypti* mosquitoes. J. Invertebr. Pathol. 68, 299–309.
Barreau, C., Jousset, F.X., Bergoin, M., 1997. Venereal and vertical transmission of the *Aedes albopictus* parvovirus in *Aedes aegypti* mosquitoes. Am. J. Trop. Med. Hyg. 57, 126–131.
Becnel, J.J., Pridgeon, J.W., 2011. Susceptibility of mosquito and lepidopteran cell lines to the mosquito iridescent virus (IIV-3) from *Aedes taeniorhynchus*. J. Invertebr. Pathol. 108, 40–45.
Bergoin, M., Tijssen, P., 2010. Densoviruses: a highly diverse group of arthropod parvoviruses. In: Asgari, S., Johnson, K.N. (Eds.), Insect Virology. Caister Academic Press, Norfolk, UK, pp. 59–82.
Bhatt, S., Gething, P.W., Brady, O.J., Messina, J.P., Farlow, A.W., Moyes, C.L., Drake, J.M., Brownstein, J.S., Hoen, A.G., Sankoh, O., Myers, M.F., George, D.B., Jaenisch, T., Wint, G.R., Simmons, C.P., Scott, T.W., Farrar, J.J., Hay, S.I., 2013. The global distribution and burden of dengue. Nature 496, 504–507.
Bian, G., Xu, Y., Lu, P., Xie, Y., Xi, Z., 2010. The endosymbiotic bacterium *Wolbachia* induces resistance to dengue virus in *Aedes aegypti*. PLoS Pathog. 6, e1000833.
Blagrove, M.S., Arias-Goeta, C., Failloux, A.B., Sinkins, S.P., 2012. *Wolbachia* strain *w*Mel induces cytoplasmic incompatibility and blocks dengue transmission in *Aedes albopictus*. Proc. Natl. Acad. Sci. USA 109, 255–260.
Blagrove, M.S.C., Arias-Goeta, C., Di Genua, C., Failloux, A.-B., Sinkins, S.P., 2013. A *Wolbachia w*Mel transinfection in *Aedes albopictus* is not detrimental to host fitness and inhibits Chikungunyav Virus. PLoS Negl. Trop. Dis. 7, e2152.
Blair, C.D., Olson, K.E., 2015. The role of RNA interference (RNAi) in arbovirus-vector interactions. Viruses 7, 820–843.
Boublik, Y., Jousset, F.X., Bergoin, M., 1994. Complete nucleotide sequence and genomic organization of the Aedes albopictus parvovirus (AaPV) pathogenic for *Aedes aegypti* larvae. Virology 200, 752–763.
Bouyer, J., Lefrançois, T., 2014. Boosting the sterile insect technique to control mosquitoes. Trends Parasitol. 30, 271–273.
Bouyer, J., Chandre, F., Gilles, J., Baldet, T., 2016. Alternative vector control methods to manage the Zika virus outbreak: more haste, less speed. Lancet Glob. Health 4, e364.
Brackney, D.E., Scott, J.C., Sagawa, F., Woodward, J.E., Miller, N.A., Schilkey, F.D., Mudge, J., Wilusz, J., Olson, K.E., Blair, C.D., Ebel, G.D., 2010. C6/36 *Aedes albopictus* cells have a dysfunctional antiviral RNA interference response. PLoS Negl. Trop. Dis. 4, e856.
Brennan, L.J., Haukedal, J.A., Earle, J.C., Keddie, B., Harris, H.L., 2012. Disruption of redox homeostasis leads to oxidative DNA damage in spermatocytes of *Wolbachia*-infected *Drosophila simulans*. Insect Mol. Biol. 21, 510–520.
Bronkhorst, A.W., van Cleef, K.W., Vodovar, N., İnce, İ.A., Blanc, H., Vlak, J.M., Saleh, M.-C., van Rij, R.P., 2012. The DNA virus Invertebrate iridescent virus 6 is a target of the *Drosophila* RNAi machinery. Proc. Natl. Acad. Sci. USA 109, E3604–E3613.
Buchatsky, L., Lebedinets, N., Kononko, G., 1997. Densonucleosis of Bloodsucking Mosquitoes: Student Handbook for Biology Majors. Taras Shevchenko'Kiev National University, Kiev.
Cammisa-Parks, H., Cisar, L.A., Kane, A., Stollar, V., 1992. The complete nucleotide sequence of cell fusing agent (CFA): homology between the nonstructural proteins encoded by CFA and the nonstructural proteins encoded by arthropod-borne flaviviruses. Virology 189, 511–524.
Carlson, J., Suchman, E., Buchatsky, L., 2006. Densoviruses for control and genetic manipulation of mosquitoes. Adv. Virus Res 68, 361–392.
Chen, S., Cheng, L., Zhang, Q., Lin, W., Lu, X., Brannan, J., Zhou, Z.H., Zhang, J., 2004.

Genetic, biochemical, and structural characterization of a new densovirus isolated from a chronically infected *Aedes albopictus* C6/36 cell line. Virology 318, 123–133.
Coon, K.L., Brown, M.R., Strand, M., 2016. Mosquitoes host communities of bacteria that are essential for development but vary greatly between local habitats. Mol. Ecol. 25, 5806–5826.
Crooks, G.E., Hon, G., Chandonia, J.M., Brenner, S.E., 2004. WebLogo: a sequence logo generator. Genome Res. 14, 1188–1190.
Dutra, H.L., Rocha, M.N., Dias, F.B., Mansur, S.B., Caragata, E.P., Moreira, L.A., 2016. *Wolbachia* blocks currently circulating Zika virus isolates in Brazilian *Aedes aegypti* mosquitoes. Cell Host Microbe 19, 771–774.
Eid, J., Fehr, A., Gray, J., Luong, K., Lyle, J., Otto, G., Peluso, P., Rank, D., Baybayan, P., Bettman, B., Bibillo, A., Bjornson, K., Chaudhuri, B., Christians, F., Cicero, R., Clark, S., Dalal, R., Dewinter, A., Dixon, J., Foquet, M., Gaertner, A., Hardenbol, P., Heiner, C., Hester, K., Holden, D., Kearns, G., Kong, X., Kuse, R., Lacroix, Y., Lin, S., Lundquist, P., Ma, C., Marks, P., Maxham, M., Murphy, D., Park, I., Pham, T., Phillips, M., Roy, J., Sebra, R., Shen, G., Sorenson, J., Tomaney, A., Travers, K., Trulson, M., Vieceli, J., Wegener, J., Wu, D., Yang, A., Zaccarin, D., Zhao, P., Zhong, F., Korlach, J., Turner, S., 2009. Real-time DNA sequencing from single polymerase molecules. Science 323, 133–138.
Faust, E.A., Ward, D.C., 1979. Incomplete genomes of the parvovirus minute virus of mice: selective conservation of genome termini, including the origin for DNA replication. J. Virol. 32, 276–292.
Frentiu, F.D., Robinson, J., Young, P.R., McGraw, E.A., O'Neill, S.L., 2010. *Wolbachia*-mediated resistance to dengue virus infection and death at the cellular level. PLoS One 5, e13398.
Gloria-Soria, A., Chiodo, T.G., Powell, J.R., 2018. Lack of evidence for natural *Wolbachia* infections in *Aedes aegypti* (Diptera: culicidae). J. Med. Entomol. 55, 1354–1356.
Goic, B., Stapleford, K.A., Frangeul, L., Doucet, A.J., Gausson, V., Blanc, H., Schemmel-Jofre, N., Cristofari, G., Lambrechts, L., Vignuzzi, M., Saleh, M.C., 2016. Virus-derived DNA drives mosquito vector tolerance to arboviral infection. Nat. Commun. 7, 12410.
Graham, R.I., Grzywacz, D., Mushobozi, W.L., Wilson, K., 2012. *Wolbachia* in a major African crop pest increases susceptibility to viral disease rather than protects. Ecol. Lett. 15, 993–1000.
Hedges, L.M., Brownlie, J.C., O'Neill, S.L., Johnson, K.N., 2008. *Wolbachia* and virus protection in insects. Science 322, 702.
Hilgenboecker, K., Hammerstein, P., Schlattmann, P., Telschow, A., Werren, J.H., 2008. How many species are infected with *Wolbachia*? - a statistical analysis of current data. FEMS Microbiol. Lett. 281, 215–220.
Hristov, G., Krämer, M., Li, J., El-Andaloussi, N., Mora, R., Daeffler, L., Zentgraf, H., Rommelaere, J., Marchini, A., 2010. Through its nonstructural protein NS1, Parvovirus H-1 induces apoptosis via accumulation of reactive oxygen species. J. Virol. 84, 5909–5922.
van den Hurk, A.F., Hall-Mendelin, S., Pyke, A.T., Frentiu, F.D., McElroy, K., Day, A., Higgs, S., O'Neill, S.L., 2012. Impact of *Wolbachia* on infection with chikungunya and yellow fever viruses in the mosquito vector *Aedes aegypti*. PLoS Negl. Trop. Dis. 6, e1892.
Hussain, M., Asgari, S., 2010. Functional analysis of a cellular microRNA in insect host-ascovirus interaction. J. Virol. 84, 612–620.
Hussain, M., Taft, R.J., Asgari, S., 2008. An insect virus-encoded microRNA regulates viral replication. J. Virol. 82, 9164–9170.
Hussain, M., Lu, G., Torres, S., Edmonds, J.H., Kay, B.H., Khromykh, A.A., Asgari, S., 2013a. Effect of *Wolbachia* on replication of West Nile virus in a mosquito cell line and adult mosquitoes. J. Virol. 87, 851–858.
Hussain, M., O'Neill, S.L., Asgari, S., 2013b. *Wolbachia* interferes with the intracellular distribution of Argonaute 1 in the dengue vector *Aedes aegypti* by manipulating the host microRNAs. RNA Biol. 10, 1868–1875.
Hussain, M., Etebari, K., Asgari, S., 2016. Functions of small RNAs in mosquitoes. In: Raikhel, A.S. (Ed.), Advances in Insect Physiology. Academic Press, pp. 189–222.
Ishizu, H., Iwasaki, Y.W., Hirakata, S., Ozaki, H., Iwasaki, W., Siomi, H., Siomi, M.C., 2015. Somatic primary piRNA biogenesis driven by cis-acting RNA elements and trans-acting Yb. Cell Rep. 12, 429–440.
Iturbe-Ormaetxe, I., Woolfit, M., Rances, E., Duplouy, A., O'Neill, S.L., 2011. A simple protocol to obtain highly pure Wolbachia endosymbiont DNA for genome sequencing. J. Microbiol Methods 84, 134–136.
Jayachandran, B., Hussain, M., Asgari, S., 2012a. RNA interference as a cellular defense mechanism against the DNA virus baculovirus. J. Virol. 86, 13729–13734.
Jayachandran, B., Hussain, M., Asgari, S., 2012b. RNA interference as a cellular defense mechanism against the DNA virus baculovirus. J. Virol. 86, 13729–13734.
Jenkins, G.M., Rambaut, A., Pybus, O.G., Holmes, E.C., 2002. Rates of molecular evolution in RNA viruses: a quantitative phylogenetic analysis. J. Mol. Evol. 54, 156–165.
Jeyaprakash, A., Hoy, M.A., 2000. Long PCR improves *Wolbachia* DNA amplification: wsp sequences found in 76% of sixty-three arthropod species. Insect Mol. Biol. 9, 393–405.
Johnson, R.M., Rasgon, J.L., 2018. Densonucleosis viruses ('densoviruses') for mosquito and pathogen control. Curr. Opin. Insect Sci. 28, 90–97.
Joubert, D.A., O'Neill, S.L., 2017. Comparison of stable and transient *Wolbachia* infection models in *Aedes aegypti* to block dengue and West Nile viruses. PLoS Negl. Trop. Dis. 11, e0005275.
Joubert, D.A., Walker, T., Carrington, L.B., De Bruyne, J.T., Kien, D.H., Hoang Nle, T., Chau, N.V., Iturbe-Ormaetxe, I., Simmons, C.P., O'Neill, S.L., 2016. Establishment of a *Wolbachia* superinfection in *Aedes aegypti* mosquitoes as a potential approach for future resistance management. PLoS Pathog. 12, e1005434.
Jousset, F.X., Barreau, C., Boublik, Y., Cornet, M., 1993. A parvo-like virus persistently infecting a C6/36 clone of *Aedes albopictus* mosquito cell line and pathogenic for *Aedes aegypti* larvae. Virus Res. 29, 99–114.
Juliano, S.A., Lounibos, L.P., 2005. Ecology of invasive mosquitoes: effects on resident species and on human health. Ecol. Lett. 8, 558–574.
Karamipour, N., Fathipour, Y., Talebi, A.A., Asgari, S., Mehrabadi, M., 2018. Small interfering RNA pathway contributes to antiviral immunity in *Spodoptera frugiperda* (Sf9) cells following Autographa californica multiple nucleopolyhedrovirus infection. Insect Biochem. Mol. Biol. 101, 24–31.
Kemp, C., Mueller, S., Goto, A., Barbier, V., Paro, S., Bonnay, F., Dostert, C., Troxler, L., Hetru, C., Meignin, C., Pfeffer, S., Hoffmann, J.A., Imler, J.L., 2013. Broad RNA interference-mediated antiviral immunity and virus-specific inducible responses in *Drosophila*. J. Immunol. 190, 650–658.
Kittayapong, P., Baisley, K.J., O'Neill, S.L., 1999. A mosquito densovirus infecting *Aedes aegypti* and *Aedes albopictus* from Thailand. Am. J. Trop. Med. Hyg. 61, 612–617.
Ledermann, J.P., Suchman, E.L., Black, W.Ct, Carlson, J.O., 2004. Infection and pathogenicity of the mosquito densoviruses AeDNV, HeDNV, and APeDNV in *Aedes aegypti* mosquitoes (Diptera: culicidae). J. Econ. Entomol. 97, 1828–1835.
Lu, P., Bian, G., Pan, X., Xi, Z., 2012. *Wolbachia* induces density-dependent inhibition to dengue virus in mosquito cells. PLoS Negl. Trop. Dis. 6, e1754.
Marina, C.F., Arredondo-Jimenez, J.I., Castillo, A., Williams, T., 1999. Sublethal effects of iridovirus disease in a mosquito. Oecologia 119, 383–388.
Marina, C.F., Ibarra, J.E., Arredondo-Jimenez, J.I., Fernandez-Salas, I., Valle, J., Williams, T., 2003. Sublethal iridovirus disease of the mosquito *Aedes aegypti* is due to viral replication not cytotoxicity. Med Vet. Entomol. 17, 187–194.
Maringer, K., Yousuf, A., Heesom, K.J., Fan, J., Lee, D., Fernandez-Sesma, A., Bessant, C., Matthews, D.A., Davidson, A.D., 2017. Proteomics informed by transcriptomics for characterising active transposable elements and genome annotation in *Aedes aegypti*. BMC Genom. 18, 101.
Martinez, J., Longdon, B., Bauer, S., Chan, Y.S., Miller, W.J., Bourtzis, K., Teixeira, L., Jiggins, F.M., 2014. Symbionts commonly provide broad spectrum resistance to viruses in insects: a comparative analysis of *Wolbachia* strains. PLoS Pathog. 10, e1004369.
Martinez, J., Tolosana, I., Ok, S., Smith, S., Snoeck, K., Day, J.P., Jiggins, F.M., 2017. Symbiont strain is the main determinant of variation in Wolbachia-mediated protection against viruses across *Drosophila* species. Mol. Ecol. 26, 4072–4084.
Mayoral, J.G., Etebari, K., Hussain, M., Khromykh, A.A., Asgari, S., 2014a. *Wolbachia* infection modifies the profile, shuttling and structure of microRNAs in a mosquito cell line. PLoS One 9, e96107.
Mayoral, J.G., Hussain, M., Joubert, D.A., Iturbe-Ormaetxe, I., O'Neill, S.L., Asgari, S., 2014b. *Wolbachia* small noncoding RNAs and their role in cross-kingdom communications. Proc. Natl. Acad. Sci. USA 111, 18721–18726.
Miesen, P., Girardi, E., van Rij, R.P., 2015. Distinct sets of PIWI proteins produce arbovirus and transposon-derived piRNAs in *Aedes aegypti* mosquito cells. Nucleic Acids Res. 43, 6545–6556.
Miesen, P., Ivens, A., Buck, A.H., van Rij, R.P., 2016a. Small RNA profiling in dengue virus 2-infected *Aedes* mosquito cells reveals viral piRNAs and novel host miRNAs. PLoS Negl. Trop. Dis. 10, e0004452.
Miesen, P., Joosten, J., van Rij, R.P., 2016b. PIWIs go viral: arbovirus-derived piRNAs in vector mosquitoes. PLoS Pathog. 12, e1006017.
Morazzani, E.M., Wiley, M.R., Murreddu, M.G., Adelman, Z.N., Myles, K.M., 2012. Production of virus-derived ping-pong-dependent piRNA-like small RNAs in the mosquito soma. PLoS Pathog. 8, e1002470.
Moreira, L.A., Iturbe-Ormaetxe, I., Jeffery, J.A., Lu, G., Pyke, A.T., Hedges, L.M., Rocha, B.C., Hall-Mendelin, S., Day, A., Riegler, M., Hugo, L.E., Johnson, K.N., Kay, B.H., McGraw, E.A., van den Hurk, A.F., Ryan, P.A., O'Neill, S.L., 2009. A *Wolbachia* symbiont in *Aedes aegypti* limits infection with dengue, Chikungunya, and *Plasmodium*. Cell 139, 1268–1278.
Mosimann, A.L.P., Bordignon, J., Mazzarotto, G.C.A., Motta, M.C.M., Hoffmann, F., Santos, C.N.Dd, 2011. Genetic and biological characterization of a densovirus isolate that affects dengue virus infection. Mem. Inst. Oswaldo Cruz 106, 285–292.
O'Neill, S.L., Kittayapong, P., Braig, H.R., Andreadis, T.G., Gonzalez, J.P., Tesh, R.B., 1995. Insect densoviruses may be widespread in mosquito cell lines. J. Gen. Virol. 76, 2067–2074.
O'Neill, S.L., Pettigrew, M.M., Sinkins, S.P., Braig, H.R., Andreadis, T.G., Tesh, R.B., 1997. *In vitro* cultivation of *Wolbachia pipientis* in an *Aedes albopictus* cell line. Insect Mol. Biol. 6, 33–39.
Osborne, S.E., Iturbe-Ormaetxe, I., Brownlie, J.C., O'Neill, S.L., Johnson, K.N., 2012. Antiviral protection and the importance of *Wolbachia* density and tissue tropism in *Drosophila simulans*. Appl. Environ. Microbiol. 78, 6922–6929.
Parry, R., Asgari, S., 2018. Aedes anphevirus: an insect-specific virus distributed worldwide in *Aedes aegypti* mosquitoes that has complex interplays with *Wolbachia* and dengue virus infection in cells. J. Virol. 92 (e00224-18).
Paterson, A., Robinson, E., Suchman, E., Afanasiev, B., Carlson, J., 2005. Mosquito densonucleosis viruses cause dramatically different infection phenotypes in the C6/36 *Aedes albopictus* cell line. Virology 337, 253–261.
Peleg, J., 1968. Growth of arboviruses in monolayers from subcultured mosquito embryo cells. Virology 35, 617–619.
Poirier, E.Z., Goic, B., Tome-Poderti, L., Frangeul, L., Boussier, J., Gausson, V., Blanc, H., Vallet, T., Loyd, H., Levi, L.I., Lanciano, S., Baron, C., Merkling, S.H., Lambrechts, L., Mirouze, M., Carpenter, S., Vignuzzi, M., Saleh, M.C., 2018. Dicer-2-dependent generation of viral DNA from defective genomes of RNA viruses modulates antiviral immunity in insects. Cell Host Microbe 23, 353–365 (e358).
Pudney, M., Varma, M., Leake, C., 1979. Establishment of cell lines from larvae of culicine (*Aedes* species) and anopheline mosquitoes. Tissue Cult. Assoc. Man. 5, 997–1002.
Ren, X., Hoiczyk, E., Rasgon, J.L., 2008. Viral paratransgenesis in the malaria vector *Anopheles gambiae*. PLoS Pathog. 4, e1000135.
Ridley, A.W., Hereward, J.P., Daglish, G.J., Raghu, S., McCulloch, G.A., Walter, G.H., 2016. Flight of *Rhyzopertha dominica* (Coleoptera: Bostrichidae)-a spatio-temporal

analysis with pheromone trapping and population genetics. J. Econ. Entomol. 109, 2561–2571.
Roekring, S., Flegel, T.W., Malasit, P., Kittayapong, P., 2006. Challenging successive mosquito generations with a densonucleosis virus yields progressive survival improvement but persistent, innocuous infections. Dev. Comp. Immunol. 30, 878–892.
Sabin, L.R., Zheng, Q., Thekkat, P., Yang, J., Hannon, G.J., Gregory, B.D., Tudor, M., Cherry, S., 2013. Dicer-2 processes diverse viral RNA species. PLoS One 8, e55458.
Schnettler, E., Donald, C.L., Human, S., Watson, M., Siu, R.W., McFarlane, M., Fazakerley, J.K., Kohl, A., Fragkoudis, R., 2013. Knockdown of piRNA pathway proteins results in enhanced Semliki Forest virus production in mosquito cells. J. Gen. Virol. 94, 1680–1689.
Schnettler, E., Sreenu, V.B., Mottram, T., McFarlane, M., 2016. *Wolbachia* restricts insect-specific flavivirus infection in *Aedes aegypti* cells. J. Gen. Virol. 97, 3024–3029.
Scott, J.C., Brackney, D.E., Campbell, C.L., Bondu-Hawkins, V., Hjelle, B., Ebel, G.D., Olson, K.E., Blair, C.D., 2010. Comparison of dengue virus type 2-specific small RNAs from RNA interference-competent and -incompetent mosquito cells. PLoS Negl. Trop. Dis. 4, e848.
Shackelton, L.A., Parrish, C.R., Truyen, U., Holmes, E.C., 2005. High rate of viral evolution associated with the emergence of carnivore parvovirus. Proc. Natl. Acad. Sci. USA 102, 379–384.
Singh, K.R.P., 1967. Cell cultures derived from larvae of *Aedes albopictus* (Skuse) and *Aedes aegypti* (L.). Curr. Sci. 36, 506–508.
Sinkins, S.P., Braig, H.R., O'Neill, S.L., 1995. *Wolbachia* superinfections and the expression of cytoplasmic incompatibility. Proc. Biol. Sci. 261, 325–330.
Son, K.N., Liang, Z., Lipton, H.L., 2015. Double-stranded RNA is detected by immunofluorescence analysis in RNA and DNA virus infections, including those by negative-stranded RNA viruses. J. Virol. 89, 9383–9392.
Teixeira, L., Ferreira, A., Ashburner, M., 2008. The bacterial symbiont *Wolbachia* induces resistance to RNA viral infections in *Drosophila melanogaster*. PLoS Biol. 6, e2.
Terradas, G., Joubert, D.A., McGraw, E.A., 2017. The RNAi pathway plays a small part in *Wolbachia*-mediated blocking of dengue virus in mosquito cells. Sci. Rep. 7, 43847.
Varjak, M., Maringer, K., Watson, M., Sreenu, V.B., Fredericks, A.C., Pondeville, E., Donald, C.L., Sterk, J., Kean, J., Vazeille, M., Failloux, A.B., Kohl, A., Schnettler, E., 2017. *Aedes aegypti* Piwi4 is a noncanonical PIWI protein involved in antiviral responses. mSphere 2 (e00144-17).
Vodovar, N., Bronkhorst, A.W., van Cleef, K.W., Miesen, P., Blanc, H., van Rij, R.P., Saleh, M.C., 2012. Arbovirus-derived piRNAs exhibit a ping-pong signature in mosquito cells. PLoS One 7, e30861.
Walker, T., Johnson, P.H., Moreira, L.A., Iturbe-Ormaetxe, I., Frentiu, F.D., McMeniman, C.J., Leong, Y.S., Dong, Y., Axford, J., Kriesner, P., Lloyd, A.L., Ritchie, S.A., O'Neill, S.L., Hoffmann, A.A., 2011. The *w*Mel *Wolbachia* strain blocks dengue and invades caged *Aedes aegypti* populations. Nature 476, 450–453.
Wang, Y., Jin, B., Liu, P., Li, J., Chen, X., Gu, J., 2018. piRNA profiling of dengue virus type 2-infected Asian Tiger mosquito and midgut tissues. Viruses 10, E213.
Weber, F., Wagner, V., Rasmussen, S.B., Hartmann, R., Paludan, S.R., 2006. Double-stranded RNA is produced by positive-strand RNA viruses and DNA viruses but not in detectable amounts by negative-strand RNA viruses. J. Virol. 80, 5059–5064.
Whitfield, Z.J., Dolan, P.T., Kunitomi, M., Tassetto, M., Seetin, M.G., Oh, S., Heiner, C., Paxinos, E., Andino, R., 2017. The diversity, structure, and function of heritable adaptive immunity sequences in the *Aedes aegypti* genome. Curr. Biol. 27, 3511–3519 (e3517).
Wise de Valdez, M.R., Suchman, E.L., Carlson, J.O., Black, W.C., 2010. A large scale laboratory cage trial of Aedes densonucleosis virus (AeDNV). J. Med. Entomol. 47, 392–399.
Wong, Z.S., Brownlie, J.C., Johnson, K.N., 2015. Oxidative stress correlates with *Wolbachia*-mediated antiviral protection in *Wolbachia-Drosophila* associations. Appl. Environ. Microbiol. 81, 3001–3005.
Ye, Y.H., Carrasco, A.M., Frentiu, F.D., Chenoweth, S.F., Beebe, N.W., van den Hurk, A.F., Simmons, C.P., O'Neill, S.L., McGraw, E.A., 2015. *Wolbachia* reduces the transmission potential of dengue-infected *Aedes aegypti*. PLoS Negl. Trop. Dis. 9, e0003894.
Zakrzewski, M., Rašić, G., Darbro, J., Krause, L., Poo, Y.S., Filipović, I., Parry, R., Asgari, S., Devine, G., Suhrbier, A., 2018. Mapping the virome in wild-caught *Aedes aegypti* from Cairns and Bangkok. Sci. Rep. 8, 4690.
Zhai, Y.-g., Lv, X.-j., Sun, X.-h., Fu, S.-h., Fen, Y., Tong, S.-x., Wang, Z.-x., Tang, Q., Attoui, H., Liang, G.-d., 2008. Isolation and characterization of the full coding sequence of a novel densovirus from the mosquito *Culex pipiens pallens*. J. Gen. Virol. 89, 195–199.
Zhang, G., Etebari, K., Asgari, S., 2016. *Wolbachia* suppresses cell fusing agent virus in mosquito cells. J. Gen. Virol. 97, 3427–3432.
Zhou, W., Rousset, F., O'Neil, S., 1998. Phylogeny and PCR-based classification of *Wolbachia* strains using wsp gene sequences. Proc. Biol. Sci. 265, 509–515.